JOURNAL OF Materials CHEMISTRY

Poly(vinylidene fluoride) with grafted 4-vinylpyridine polymer side chains for pH-sensitive microfiltration membranes

Guangqun Zhai, Lei Ying, E. T. Kang* and K. G. Neoh

Department of Chemical and Environmental Engineering, National University of Singapore, Kent Ridge, Singapore 119260. E-mail: cheket@nus.edu.sg

Received 4th July 2002, Accepted 9th August 2002
First published as an Advance Article on the web 7th October 2002

The thermally induced molecular graft copolymerization of 4-vinylpyridine (4VP) with ozone-preactivated poly(vinylidene fluoride) (PVDF) was carried out in *N*-methyl-2-pyrrolidone (NMP) solution to produce 4VP-*g*-PVDF copolymers. The chemical composition and structure of the 4VP-*g*-PVDF copolymers were characterized by element analysis, Fourier transform infrared (FTIR) spectroscopy, and thermogravimetric analysis (TGA). In general, the graft concentration of the 4VP polymer in the 4VP-*g*-PVDF copolymer increased with the [4VP]/[PVDF] molar feed ratio used for the graft copolymerization. Microfiltration (MF) membranes were prepared by phase inversion in aqueous solutions of different pH values and from copolymers of different graft concentrations. The surface composition of the copolymer MF membranes was investigated by X-ray photoelectron spectroscopy (XPS). A significant surface enrichment of the more hydrophilic 4VP side chains was observed. The surface morphology of the MF membranes was investigated by scanning electron microscopy (SEM). The pore size and pore size distribution of the 4VP-*g*-PVDF MF membranes were measured using a Coulter Porometer II apparatus. The flux of the aqueous solutions through the 4VP-*g*-PVDF MF membranes exhibited a pH-dependent behavior, due to the interactions of the pyridine groups of the grafted 4VP chains with the aqueous solutions through hydrogen bonding and protonation.

1 Introduction

Fluoropolymers, such as poly(tetrafluoroethylene) (PTFE) and poly(vinylidene fluoride) (PVDF), have been widely investigated for their unique mechanical and physicochemical properties during the past decades. Differing from the dielectric applications of PTFE, PVDF has been shown to be an excellent membrane material for chemical and biological applications.[1–6] Its piezoelectrical and pyroelectrical properties also render PVDF a material of choice for sensors.[7–9] However, the hydrophobic nature of the polymer has limited its application to some extent in certain areas. A great deal of effort has been devoted to chemical and physical modification of the PVDF membranes. The techniques used have included plasma treatment, blending with hydrophilic polymers, gamma ray irradiation, and ion beam irradiation.[10–13] A number of studies have also been devoted to the graft copolymerization of functional monomers or grafting of functional polymers onto existing PVDF membranes to improve their surface hydrophilic, antifouling and pH-sensitive properties and their biocompatibility.[14–20]

However, surface modification of existing membranes by grafting or graft copolymerization is likely to be accompanied by changes in the membrane pore dimension and pore size distribution, leading to reduced permeability.[21,22] Moreover, the extents of grafting on the membrane surfaces and the surfaces of the pores may differ considerably. Thus, the approach of molecular or bulk graft copolymerization, followed by phase inversion, to membrane fabrication may prove to be particularly useful in certain cases. For instance, uniform post-functionalization by graft copolymerization of the hollow fibre membranes and their pore surfaces is expected to be spatially difficult. Furthermore, the preparation of membranes from graft copolymers by the phase inversion technique can greatly facilitate the control of the pore size, the pore size distribution and the composition of the pore surfaces through the control of the copolymer structure and composition.

In the present work, we report on the synthesis and characterization of PVDF with 4-vinylpyridine (4VP) polymer side chains (the 4VP-*g*-PVDF copolymers) from the molecular graft copolymerization of 4VP with ozone-preactivated PVDF in *N*-methyl-2-pyrrolidone (NMP) solution. The resulting graft copolymers are shown to be promising materials for fabricating microfiltration (MF) membranes having hydrophilic properties and pH-sensitive permeability to aqueous solutions.

2 Experimental

2.1 Materials and reagents

PVDF (Kynar K-761) powders (MW = 441000) were obtained from Elf Atochem of North America Inc. The solvent, NMP (reagent grade), was obtained from Merck Chemical Co. They were used as received. The monomer, 4VP, of 95% purity and purchased from Aldrich Chemical Company of Milwaukee, WI, USA, was distilled under reduced pressure before use.

2.2 Ozone preactivation of PVDF and thermally induced graft copolymerization of 4VP with PVDF (4VP-*g*-PVDF copolymer)

PVDF powders were dissolved in NMP to form a 7 wt.% solution. A continuous O_3/O_2 mixture stream was bubbled through 30 mL of the PVDF/NMP solution at room temperature ($\sim$25 °C) for about 15 min. The O_3/O_2 mixture stream was generated from an Azcozon RMU16-40EM ozone generator. The flow rate was adjusted to 300 L h^{-1} to result in an ozone concentration of about 0.27 g L^{-1} in the gaseous mixture. After the ozone preactivation, the polymer solution was cooled in an ice bath. An argon stream was introduced for about 30 min to degas the ozone and oxygen dissolved in the solution. The 4VP monomer and NMP solvent were then added to achieve a specific [4VP]/[–CH_2CF_2–] molar feed ratio and to adjust the total solution to 40 mL. After an additional 15 min of argon purging, the temperature of the water bath was raised to 60 °C to induce the decomposition of peroxide groups

 DOI: 10.1039/b206486c

on the PVDF chains and to initiate the graft copolymerization of 4VP. During the 4 h of thermal graft polymerization, a constant flow of argon was maintained. After the reaction, the reaction mixture was cooled in an ice bath and the resultant 4VP-*g*-PVDF copolymer was precipitated in an excess amount of absolute ethanol (a good solvent for 4VP and its homopolymer). After filtering, the copolymer was washed in an excess volume of ethanol for 48 h. The solvent was changed every 8 h. The copolymer sample was recovered and dried by pump under reduced pressure for subsequent characterization. The processes of ozone preactivation and thermally induced graft copolymerization are shown schematically in Fig. 1.

2.3 Fabrication of the MF membranes

The MF membranes were prepared by the phase inversion technique. The 4VP-*g*-PVDF copolymer powders were dissolved in NMP to a concentration of 12 wt.% at room temperature. The copolymer solution was cast on a glass plate and the glass plate was subsequently immersed in doubly distilled water. After the membrane had detached from the glass plates, it was extracted in a second bath of doubly distilled water at 70 °C for 30 min. This procedure was to stabilize the pore structure and to refine the pore size distribution. The purified MF membrane was dried by pump under reduced pressure for subsequent characterization. The structure of the MF membranes is also shown schematically in Fig. 1.

2.4 Fourier transform infrared (FTIR) spectroscopy

After dispersion in KBr, the FTIR spectra of the homopolymer and copolymer powders were measured on a Bio-Rad FTS 135 FT-IR spectrophotometer. Each spectrum was collected by accumulating 16 scans at a resolution of 8 wavenumbers.

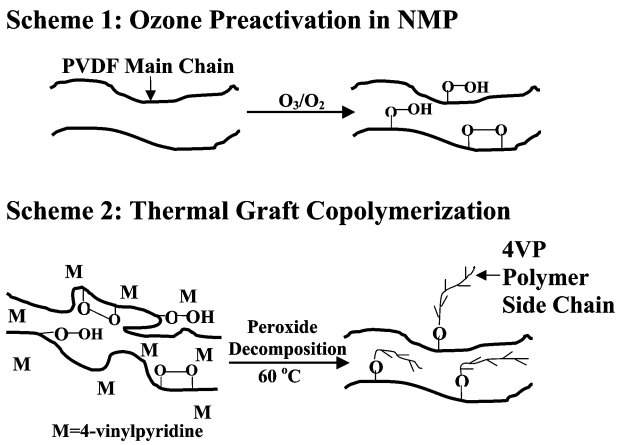

Fig. 1 Schematic illustration of the process of thermally induced graft copolymerization of 4VP on the ozone-preactivated PVDF backbones in NMP solution and the structure of the 4VP-*g*-PVDF MF membrane prepared by phase inversion.

2.5 Copolymer composition analysis

The carbon, nitrogen and hydrogen elemental contents were determined using a PerkinElmer 2400 element analyzer. Taking into account the stoichiometries of the graft and the fluoropolymer chains, the bulk graft concentration, defined as the number of 4VP repeat units per repeat unit of PVDF, or the $([–4VP–]/[–CH_2CF_2–])_{bulk}$ ratio, can be calculated from eqn. (1):

$$([–4VP–]/[–CH_2CF_2–])_{bulk} = 2[N]/([C] - 7[N]) \times 100\% \quad (1)$$

where the factors 2 and 7 are introduced to account for the fact that there are 2 and 7 carbon atoms per repeat unit of PVDF and 4VP polymer, respectively.

2.6 Scanning electron microscopy (SEM)

The surface morphology of the MF membranes was studied by SEM, using a JEOL 6320 scanning electron microscope. The membranes were mounted on the sample studs by means of double-sided adhesive tape. A thin layer of palladium was sputtered onto the membrane surface prior to the SEM measurement. The measurements were performed at an accelerating voltage of 8 kV.

2.7 Pore size measurement

The pore sizes and the pore size distributions of the 4VP-*g*-PVDF membranes were measured using a Coulter Porometer II apparatus, manufactured by Coulter Electronics Ltd., Buckinghamshire, UK. The commercial product, Porofil®, for the Coulter Porometer instrument was used as the wetting agent.

2.8 X-Ray photoelectron spectroscopy (XPS)

XPS measurements were made on a Kratos AXIS HSi spectrometer with a monochromatized Al Kα X-ray source (1486.6 eV photons) at a constant dwell time of 100 ms and a pass energy of 40 eV. The anode current was 15 mA. The pressure during the analysis was maintained at below 5×10^{-8} Torr. The polymer membranes were mounted on the sample studs by means of double-sided adhesive tape. The core-level signals were obtained at a photoelectron take-off angle (α, with respect to the sample surface) of 90°. All binding energies (E_b) were referenced to the C 1s hydrocarbon peak at 284.6 eV or the CF_2 peak of PVDF at 290.5 eV. In peak synthesis, the full width at half maximum (FWHM) of the Gaussian peaks was maintained constant for all components in a particular spectrum. Surface elemental stoichiometries were determined from peak-area ratios, after correcting with the experimentally determined sensitivity factors, and were reliable to $\pm 5\%$. The elemental sensitivity factors were determined using stable binary compounds of well-established stoichiometries.

2.9 Thermogravimetric analysis (TGA)

The thermal stability of the 4VP-*g*-PVDF copolymers was studied by TGA. The samples were heated from room temperature to about 700 °C at a rate of 10 °C min^{-1} under a dry nitrogen atmosphere in a Du Pont Thermal Analyst 2100 system, equipped with a TGA 2050 thermogravimetric thermal analyzer.

2.10 pH-dependent flux of aqueous solutions through the 4VP-*g*-PVDF MF membranes

A 4VP-*g*-PVDF MF membrane was immersed in an aqueous HCl solution of a prescribed pH value for several minutes. It was then mounted on a microfiltration cell (Toyo Roshi

UHP-25, Tokyo, Japan). An aqueous HCl solution of the same pH value was added to the cell. Sodium chloride was added to adjust the ionic strength of the aqueous solution to 0.1 mol L^{-1}. The flux was calculated from the weight of solution permeated per unit time and per unit area of the membrane surface under a nitrogen atmosphere of 0.03 kg cm^{-2}.

3 Results and discussions

3.1 Ozone pre-activation of PVDF and graft copolymerization of 4VP with PVDF (4VP-*g*-PVDF copolymer)

Ozone treatment has been widely adopted to generate the peroxide and hydroperoxide species on polymer chains and surfaces.[23–26] These functional groups can be used to initiate the free radical polymerization of vinyl monomers to produce the graft copolymers.[23] For this and other chain polymerization reactions, in general, the initiator decomposition is the rate-limiting step. The activation energy and Arrhenius coefficient (ln A) for the decomposition reaction of the initiators on the ozone-preactivated PVDF chains are reported to be about 39 kJ mol^{-1} and 5.8, respectively.[27] Thus, the value of A is about 330 s^{-1}. Based on these data, the half-life of the peroxide groups at 60 °C is calculated to be about 45 min. Thus, it is probably sufficient to fix the reaction time at 4 h for the thermally induced initiator decomposition and graft copolymerization in this work. The processes of ozone preactivation, graft copolymerization, and MF membrane fabrication are illustrated schematically in Fig. 1.

3.1.1 Composition analyses of the 4VP-*g*-PVDF copolymers. In general, the amount of peroxide groups created on the PVDF chains by the ozone pretreatment, or the initiator concentration, depends on the treatment temperature, ozone concentration and treatment time.[27] Previous studies had shown that an ozone pretreatment time of 15 min under the present experimental conditions could result in a peroxide content of about 10^{-4} mol g^{-1} of PVDF, as determined by the 2,2-diphenyl-1-picrylhydrazyl (DPPH) assay.[23] Excessive ozone pretreatment will lead to the over-oxidation and degradation (scission) of the polymer chains, especially when the treatment time is above 15 min. Thus, the ozone pretreatment time is fixed at 15 min in the present work.

For the graft copolymerization of 4VP with PVDF, the 4VP monomer feed ratio is an important parameter that can be used to regulate the graft concentration. Elemental analysis suggests that the bulk graft concentration, defined either as the $([–4VP–]/[–CH_2CF_2–])_{bulk}$ ratio or simply as the $([N]/[C])_{bulk}$ ratio, increases with the increase in the [4VP]/[$–CH_2CF_2–$] molar feed ratio used for the graft copolymerization. The bulk [N]/[C] ratio, obtained from the elemental analysis, and the corresponding bulk graft concentration, calculated from eqn. (1), as a function of the monomer feed ratio ([4VP]/[$–CH_2CF_2–$] ratio) is shown in Fig. 2. Comparison of the bulk graft concentration, or the $([–4VP–]/[–CH_2CF_2–])_{bulk}$ ratio, with the molar feed ratio in Fig. 2 indicates that the grafting efficiency decreases from about 6% to about 2% with an increase in the [4VP]/[$–CH_2CF_2–$] feed ratio from 0.61 to 3.66. This result suggests that the graft copolymerization reaction is limited by the peroxide initiator concentration, and not by monomer diffusion. Furthermore, at a low bulk graft concentration, a finite amount of PVDF homopolymer probably coexists in the grafted fraction. The removal of the PVDF homopolymer from the graft copolymers by solvent extraction will be difficult.

3.1.2 FTIR spectra of the 4VP-*g*-PVDF copolymers. The FTIR spectra of the 4VP-*g*-PVDF copolymers, obtained from different monomer feed ratios were also studied. Compared to that of the pristine PVDF and that of the 4VP homopolymer, the spectra of the 4VP-*g*-PVDF copolymers contain the characteristic absorption band for the pyridine groups (ν = 1602 cm^{-1}), associated with the grafted 4VP chains.[28] Since the concentration of a functional group is directly proportional to the absorption peak area in the FTIR spectrum, the ratio of the absorption peak area at 1602 cm^{-1} to that at 1120–1280 cm^{-1} (the absorption band associated with the CF_2 groups of PVDF[23]) is directly related to the bulk graft concentration of the 4VP side chains in the respective 4VP-*g*-PVDF copolymer. The FTIR spectroscopic results indicate that the bulk graft concentration increases with an increase in the respective [4VP]/[$–CH_2CF_2–$] molar feed ratio used for graft copolymerization. This result is in a good agreement with that obtained from the element analysis.

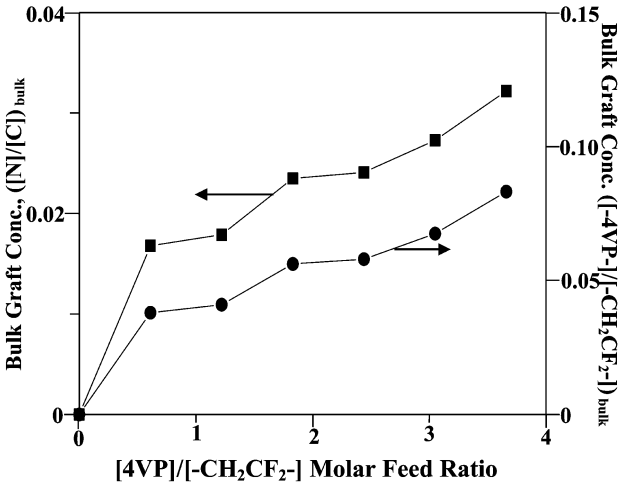

Fig. 2 Effect of [–4VP–]/[$–CH_2CF_2–$] molar feed ratio on the bulk [N]/[C] ratio and the bulk graft concentration ($[–4VP–]/[–CH_2CF_2–]_{bulk}$ ratio) of the 4VP-*g*-PVDF copolymer.

3.1.3 TGA of the 4VP-*g*-PVDF copolymers. One of the unique properties of the pristine PVDF is its outstanding thermal stability. The thermal stability of the 4VP-*g*-PVDF copolymers was studied by TGA. Fig. 3 shows the respective TGA curves of three 4VP-*g*-PVDF copolymers of different bulk graft concentrations, the pristine PVDF and the 4VP homopolymer. In comparison with the pristine PVDF and 4VP homopolymer, the 4VP-*g*-PVDF copolymers show an intermediate weight loss behavior. Differing from the two homopolymers, the 4VP-*g*-PVDF copolymers undergo a distinct two-step thermal decomposition process. The onset of the first major weight loss occurs at about 300 °C, corresponding to the

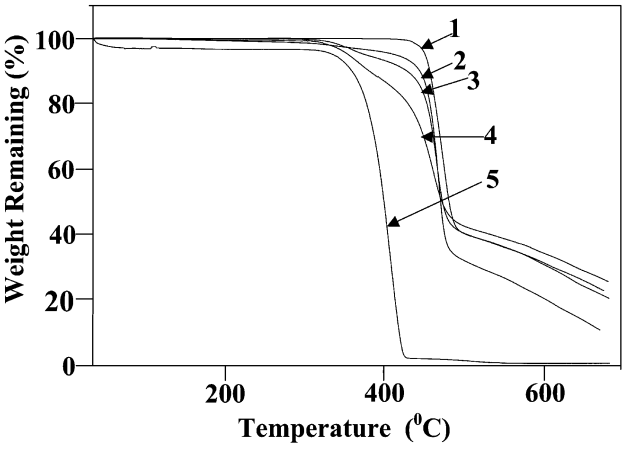

Fig. 3 TGA curves of: 1, pristine PVDF; 2–4, 4VP-*g*-PVDF copolymers of different bulk graft concentrations ($[–4VP–]/[–CH_2CF_2–]_{bulk}$ ratios), 0.038 (2), 0.068 (3) and 0.083 (4); and 5, 4VP homopolymer.

decomposition of the 4VP side chains of the copolymer. The second major weight loss commences at about 400 °C, which coincides with the thermal decomposition temperature of the PVDF main chains. The TGA curves also indicate that the extent of weight loss of the 4VP-*g*-PVDF copolymer during the first step of thermal decomposition is approximately equal to the content of the 4VP segments in the respective graft copolymer.

3.2 MF membranes fabricated from the 4VP-*g*-PVDF copolymers

After the 4VP-*g*-PVDF MF membranes were fabricated by the phase inversion technique in water and at room temperature from the 12 wt.% NMP solutions of the respective copolymers, the surface composition and morphology of the membranes were investigated by XPS and SEM, respectively.

3.2.1 XPS analysis of the 4VP-*g*-PVDF MF membranes. The C 1s core-level spectra of the membranes cast from 12 wt.% NMP solutions of the pristine PVDF, the ozone-preactivated PVDF, and the 4VP-*g*-PVDF copolymers from different molar feed ratios ([4VP]/[–CH_2CF_2–] = 0.61, 2.44, and 3.66, respectively) are shown in Fig. 4. For the pristine PVDF MF membrane, the C 1s core-level spectrum can be curve-fitted with two peak components at E_b values of about 285.8 eV and 290.5 eV, attributable to the CH_2 and CF_2 species, respectively.[23] The ratio of the two species, determined from their spectral peak area ratio after curve-fitting, is about 1.06. The ratio is in a good agreement with the theoretical ratio of 1.0 dictated by the chemical structure of PVDF. The C 1s core-level spectrum of the PVDF membrane cast from the NMP solution after 15 min of ozone pretreatment can be curve-fitted with three peak components at E_b values of about 285.8 eV, 286.2eV and 290.5 eV, attributable to the CH_2 species, the CO species created on the PVDF main chains during ozone preactivation in NMP solution, and the CF_2 species, respectively.[23] The C 1s core-level spectrum of the 4VP-*g*-PVDF MF membranes can be curve-fitted with five peak components using the following approach. The peak components of about equal intensities at about 285.8 eV and 290.5 eV are assigned to the CH_2 and CF_2 species, respectively, of the PVDF main chains of the copolymer. The peak components at about 284.6 eV and 285.5 eV are assigned to the CH and CN species of the grafted 4VP polymer side chains in the copolymers. The peak component at about 286.2 eV is assigned to the CO species.[23]

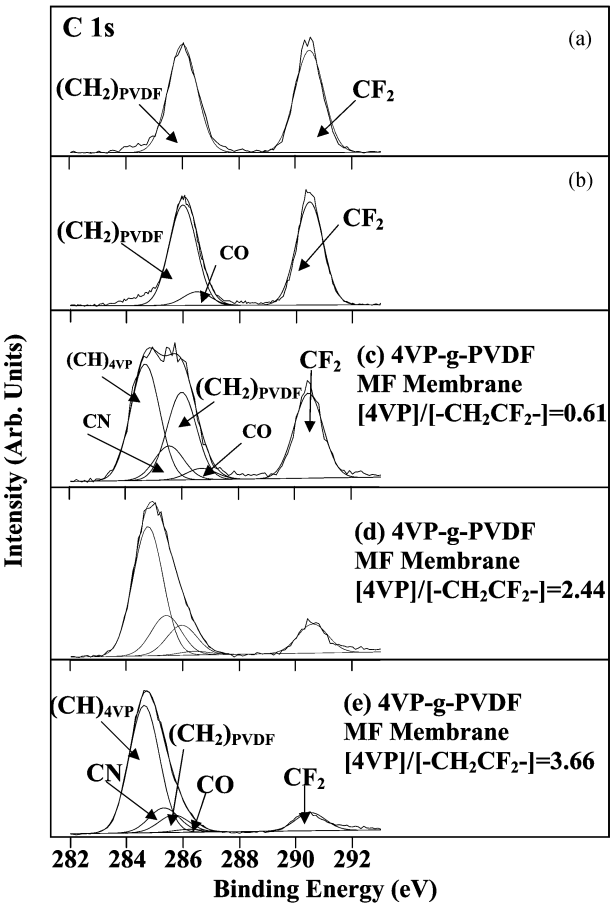

Fig. 4 XPS C 1s core-level spectra of the MF membranes cast by phase inversion from 12 wt.% NMP solutions of: (a) the pristine PVDF homopolymer; (b) the PVDF after 15 min of ozone pretreatment; and (c)–(e) the 4VP-*g*-PVDF copolymers prepared from [4VP]/[–CH_2CF_2–] molar feed ratios of 0.61 (c), 2.44 (d) and 3.66 (e).

The C 1s core-level spectra in Fig. 4 show that after ozone preactivation and graft copolymerization, the peak intensities of the $(CH_2)_{PVDF}$ and CF_2 species are reduced, especially when the [4VP]/[–CH_2CF_2–] molar feed ratios are greater than 2. The proportion of the CF_2 species, determined from the CF_2 peak component spectral area, decreases from about 48% to about 10% when the [4VP]/[–CH_2CF_2–] feed ratio used for graft copolymerization increases from 0 (the pristine PVDF MF membrane) to 3.66. In addition to the actual graft copolymerization, surface enrichment of the grafted hydrophilic 4VP side chains has to be taken into account and will be discussed in detail later. The spectra also indicate that the spectral area ratio of the $(CH)_{4VP}$ component at 284.6 eV to that of the CF_2 component at 290.5 eV increases with the increasing [4VP]/[–CH_2CF_2–] feed ratio used for graft copolymerization, consistent with the increase in the graft concentration. The surface [N]/[C] ratio for the 4VP-*g*-PVDF MF membrane is determined from the respective N 1s to C 1s core-level spectral area ratio. The surface graft concentration of the 4VP polymer on the MF membranes, or $([–4VP–]/[–CH_2CF_2–])_{surface}$ ratio, is determined from the respective [N]/[C] ratio by taking into account the elemental stoichiometries of the graft and the fluoropolymer chains, as in the case of the bulk graft concentration. Fig. 5 shows that the surface graft concentration of the 4VP polymer on the 4VP-*g*-PVDF MF membranes increases with the [4VP]/[–CH_2CF_2–] feed ratio used for graft copolymerization.

The bulk graft concentration of the copolymers (determined by element analyses) and the surface graft concentration of the corresponding MF membranes fabricated by the phase inversion process (determined by XPS analyses) are compared in Fig. 6. It is clear that the surface graft concentration is

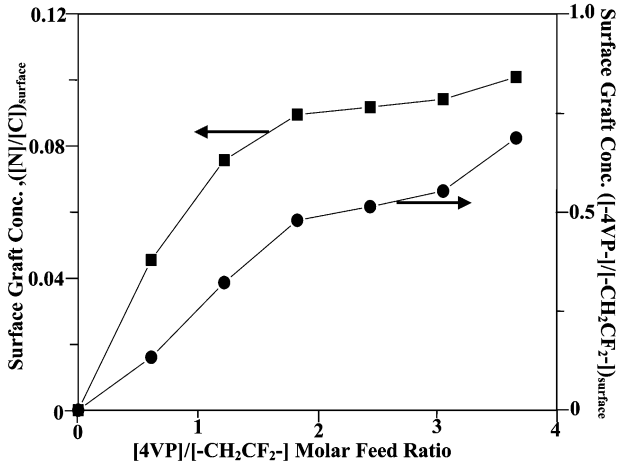

Fig. 5 Effect of [4VP]/[–CH_2CF_2–] molar feed ratio on the surface [N]/[C] ratio and the surface graft concentration ([–4VP–]/[–CH_2CF_2–]$_{surface}$ ratio) of the 4VP-*g*-PVDF MF membranes.

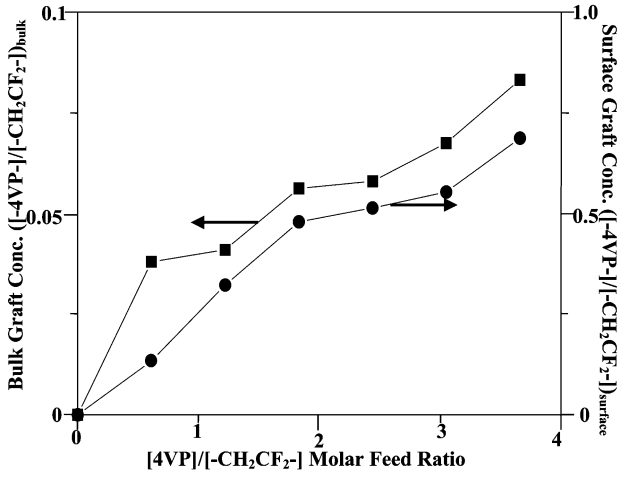

Fig. 6 Comparison between the bulk graft concentration and the surface graft concentration of the 4VP-*g*-PVDF MF membrane cast by phase inversion from the 12 wt.% NMP solution of the respective 4VP-*g*-PVDF copolymer.

always higher than the corresponding bulk graft concentration. Due to the immiscibility of the more hydrophilic 4VP polymer side chains with the hydrophobic PVDF main chains, surface enrichment of the hydrophilic component occurs in the copolymer membranes during the phase inversion process in water.

3.2.2 Surface morphology of the 4VP-*g*-PVDF MF membranes. The dependence of the surface morphology of 4VP-*g*-PVDF MF membranes on the graft concentration was investigated by SEM. The SEM images, obtained at a magnification of 5000×, for the MF membranes cast by the phase inversion technique at 25 °C from the 12 wt.% NMP solutions of the pristine PVDF powders and three 4VP-*g*-PVDF copolymers (bulk graft concentration or [–4VP–]/[–CH_2CF_2–]$_{bulk}$ = 0.038, 0.068 and 0.083, respectively) are shown in Fig. 7. The SEM results indicate that the membranes cast from the NMP solutions of the 4VP-*g*-PVDF copolymer samples have a higher porosity than that cast from the NMP

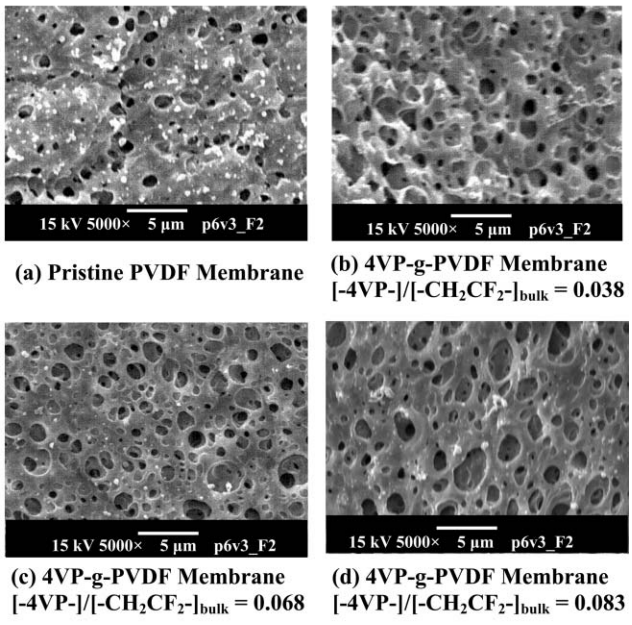

Fig. 7 SEM micrographs of the MF membranes cast by phase inversion from the 12 wt.% NMP solution of: (a) the pristine PVDF; and (b)–(d) the 4VP-*g*-PVDF copolymers of bulk graft concentrations ([–4VP–]/[–CH_2CF_2–]$_{bulk}$ ratios) of 0.038 (b), 0.068 (c) and 0.083 (d).

solution of the pristine PVDF and the pore size appears to increase with the bulk graft concentration of 4VP polymer in the copolymers. In the presence of the more hydrophilic 4VP polymer side chains, surface enrichment of the 4VP polymers takes place during phase inversion in water to maximize the interfacial interaction between the pore surface and water, resulting in an increase in the pore size. For the 4VP-*g*-PVDF MF membrane with a high graft concentration, mass migration and accumulation of the 4VP chains at the water/PVDF interface during phase inversion readily give rise to a large pore size.

3.3 Pore size measurements and pH-sensitive flux behavior through the 4VP-*g*-PVDF MF membranes

3.3.1 Pore size measurements of the 4VP-*g*-PVDF MF membranes. The pore sizes of the various 4VP-*g*-PVDF MF membranes were measured on a Coulter Porometer II apparatus using the commercial fluid Porofil® as the wetting agent. The Porofil®-wetted membrane samples were subjected to an increasing pressure from 0.1 to 8.6 kg cm^{-2} exerted by nitrogen. As the imposed pressure increases, it will reach a point at which it can overcome the surface tension of the liquid in the largest pores and will push the liquid out. The pressure is termed the minimum bubble point and corresponds to the measurement of maximum pore size. Increasing the pressure will further allow the gas to flow through smaller pores until all the pores have been emptied. The result is governed by the Washburn equation (eqn. (2)):[29]

$$P \cdot r = 2\gamma\cos\theta \quad (2)$$

where P is the pressure, r is the average pore radius of the measured membrane sample, and $\gamma\cos\theta$ is the Wilhelmy surface tension. The average pore sizes of the various MF membranes cast from the 4VP-*g*-PVDF graft copolymers of different graft concentrations are shown in Table 1. It indicates that the average pore size of the 4VP-*g*-PVDF MF membrane increases with the graft concentration of the 4VP side chains in the copolymer.

The dependence of pore size of the 4VP-*g*-PVDF MF membrane on the pH of the aqueous casting solutions is also shown in Table 1. The pore size of the 4VP-*g*-PVDF MF membrane increases with the decreasing pH value of the casting bath. Thus, a high proton concentration of the casting bath will lead to a large pore size. The phenomenon probably arises from the interaction equilibrium between the pyridine groups on the pore surfaces and the protons in the acidic solution. The pore size of the 4VP-*g*-PVDF MF membranes is also dependent on the concentration of the copolymer in the casting solution, as shown in Table 1. The pore size decreases drastically with the increase in concentration of the 4VP-*g*-PVDF copolymer in the casting solution. At a low copolymer solution concentration, the extraction of the solvent from the bulk and the polymer-solvent phase is facilitated. As a result, larger pore sizes are obtained for the 4VP-*g*-PVDF MF membranes cast from the copolymer solution of lower concentration. The pore size measurement also suggests that the pore size distribution of the 4VP-*g*-PVDF MF membranes is similar to that of the commercial PVDF MF membranes of standard diameters (d) between 0.45 μm and 0.65 μm. Thus, commercial PVDF membranes with d = 0.45 μm and d = 0.65 μm were selected as the pristine PVDF MF membranes for comparative flux studies in the present work.

3.3.2 pH-dependent flux behavior of aqueous solutions through the 4VP-*g*-PVDF MF membranes. The pH-dependent flux behavior of aqueous solutions through the 4VP-*g*-PVDF MF membranes is shown in Fig. 8. The permeability of aqueous solutions through the pristine PVDF MF membranes

Table 1 Pore size distribution of the 4VP-*g*-PVDF MF membranes[a]

Molar feed ratio [4VP]/[–CH_2CF_2–]	Bulk graft concentration [–4VP–]/[–CH_2CF_2–]	pH of casting bath	Concentration of casting solution (wt.%)	Min pore size/μm	Max pore size/μm	Mean pore size/μm
Effect of bulk graft concentration on the pore-size distribution[b]						
0.61	0.038	6	12	0.23	2.l4	0.95
1.02	0.041	6	12	0.33	2.84	1.03
1.83	0.056	6	12	0.26	2.94	1.08
2.44	0.058	6	12	0.37	2.14	1.23
3.05	0.068	6	12	0.39	2.28	1.31
3.66	0.083	6	12	0.48	3.62	1.38
Effect of pH value of the casting bath on the pore-size distribution[c]						
3.05	0.068	6	12	0.85	3.18	1.38
3.05	0.068	4	12	0.89	2.84	1.50
3.05	0.068	2	12	0.83	2.55	1.54
3.05	0.068	1	12	0.39	4.16	1.67
Effect of solution concentration on the pore-size distribution[d]						
2.44	0.058	6	10	0.23	2.52	1.83
2.44	0.058	6	12	0.37	2.14	1.23
2.44	0.058	6	15	0.16	0.72	0.22

[a]For the commercial PVDF membranes with standard pore diameters d = 0.45 and 0.65 μm. PVDF (d = 0.45 μm): max pore size = 1.86 μm, min pore size = 1.17 μm, mean pore size = 1.41 μm. PVDF (d = 0.65 μm): max pore size = 2.40 μm, min pore size = 1.42 μm, mean pore size = 1.96 μm. [b]Cast in doubly distilled water. [c]Cast in aqueous HCl solution with a specific pH value; sodium chloride is added to fix the ionic strength of the casting bath at 0.1 mol L^{-1}. [d]Cast in doubly distilled water.

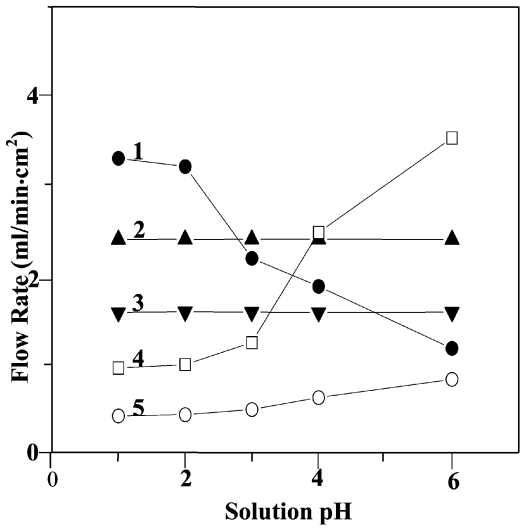

Fig. 8 pH-dependent permeability of aqueous solution through the AAc-*g*-PVDF, pristine PVDF and 4VP-*g*-PVDF MF membranes. Curve 1 is from the flux through the AAc-*g*-PVDF MF membrane (average pore size 1.52 μm, surface graft concentration ([–AAc–]/[–CH_2CF_2–]$_{surface}$) = 0.97).[23] Curves 2 and 3 are from fluxes through the commercial PVDF membranes (standard pore diameter: d = 0.65 and 0.45 μm, respectively, and with characteristic pore size distribution similar to those of 4VP-*g*-PVDF copolymer membranes). Curves 4 and 5 are obtained from two 4VP-*g*-PVDF MF membranes with surface graft concentrations ([–4VP–]/[–CH_2CF_2–]$_{surface}$) of 0.55 and 0.13, respectively.

is pH-independent (curves 2 and 3). On the other hand, the flux of the aqueous solution through the 4VP-*g*-PVDF MF membranes exhibits a pH-dependent behavior. The permeation rate increases with increasing solution pH from 1 to 6 (curves 4 and 5). The pH-dependent flux behavior is opposite to that of the MF membranes prepared from PVDF with poly(acrylic acid) grafted side chains (curve 1).[23] Furthermore, the sensitivity of the pH-dependent change in flux of the aqueous solution through the 4VP-*g*-PVDF MF membrane is enhanced by an increase in the 4VP polymer graft concentration.

The change in permeability or flux in response to the change in solution pH can be attributed to the change in conformations of the graft chains on the membrane surface, especially on the pore surfaces. Due to the non-ionizablity of the polymer chains in the pristine PVDF MF membranes, the polymer chain conformation and the membrane pore dimension will remain constant at all pH values. On the other hand, as a weak base, the pyridine groups of the grafted 4VP side chains are protonated and become complexed in an acid solution. The resulting ionic character and the electrostatic repulsion among the positively charged pyridinium nitrogen atoms overcome the hydrophobic interactions among the alkyl segments of the chains. The uncoiling of the polymer side chains and their interactions with the aqueous solution lead to an extended conformation in the pores.[30] As a result, the effective pore dimension, and thus the permeability of the aqueous solution through the MF membrane, is reduced.

The present pH-dependent flux results for the aqueous solution differ from the pH-dependent flux behavior of the aqueous solution through the MF membrane prepared from PVDF with grafted acid polymer side chains, in particular, the PVDF with grafted poly(acrylic acid) side chains (AAc-*g*-PVDF copolymers).[23] As a weak acid (pK_a = 4.3), the carboxylic groups of the AAc-*g*-PVDF copolymer can be ionized, or deprotonated, readily to become negatively charged. With increasing pH values (pH > 3) of the solution, most of the carboxylic groups are transformed into carboxylic ions. Strong electrostatic repulsion among the carboxylic ions, together with their strong interaction with the aqueous solution, forces the AAc polymer side chains to adopt a highly extended conformation. The extension of the AAc polymer side chains into the pores reduces the effective pore dimension, and results in the reduced permeability of the aqueous solution of high pH value through the AAc-*g*-PVDF MF membrane.[23] Thus, the present 4VP-*g*-PVDF MF membranes, prepared from PVDF with grafted basic polymer (4VP polymer) side chains, complement the AAc-*g*-PVDF MF membranes in regulating the flux of the aqueous solutions in the pH range 1–7.

3.4 Interaction of the 4VP polymer with protonic acids

For the nitrogen-containing species, such as pyridine and imidazole, hydrogen bonding with proton-donating species, such as phenols, carboxylic acids, inorganic acids and water, occurs readily.[31–36] Thus, the pyridine groups of the grafted 4VP side chains can become involved in two types of interaction in acidic solutions, *viz.*, hydrogen bonding and pyridine protonation, that lead to the observed pH-dependent flux of the aqueous solutions through the 4VP-*g*-PVDF MF

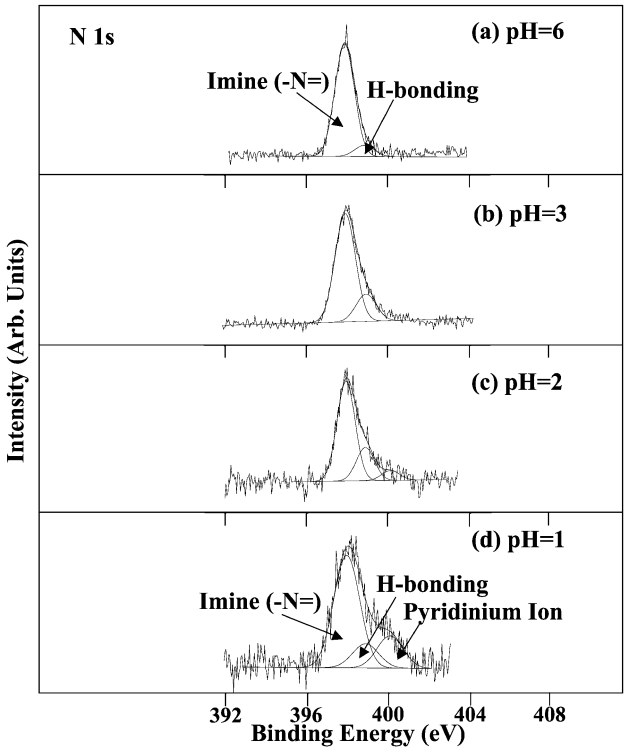

Fig. 9 XPS N 1s core-level spectra of four MF membranes cast by phase inversion from a 12 wt.% NMP solution of the 4VP-*g*-PVDF copolymer ($[–4VP–]/[–CH_2CF_2–]_{surface}$ = 0.55) and after being immersed for 5 min in aqueous solutions of different pH values: (a) pH = 6, (b) pH = 3, (c) pH = 2, and (d) pH = 1

membrane. In order to investigate the interaction of the 4VP side chains in the acid solutions, XPS was employed to study the variation in the chemical state of the elemental nitrogen of the pyridine group after the 4VP-*g*-PVDF MF membrane has been exposed to acidic solutions of different pH values for 5 min. The N 1s core-level spectra of the resulting membranes are shown in Fig. 9. The XPS spectra can be curve-fitted with three components using the following approaches. The main peak component at about 398.5 eV is assigned to the imine (–N=) moiety of the pyridine rings, the peak component at about 399.5 eV is assigned to the hydrogen-bonded imine, and the peak component at about 400.8 eV is assigned to the protonated pyridinium ions.[37–39] The latter species has been reported to undergo a positive E_b shift of 2.1–2.5 eV from the neutral pyridine nitrogen.[37,39] The N 1s spectra in Fig. 9 clearly indicate that, when the proton concentration is low, or when the pH value is higher than 2, the main form of interaction is hydrogen bonding. The percentage of N atoms involved in the hydrogen bonding increases from 9% to 21% when the pH value of the solution decreases from 6 to 3. When the pH value of the solution is decreased to 2, protonation of pyridine becomes significant. The percentages of imine groups involved in hydrogen bonding and protonation are about 21% and 7%, respectively. When the solution pH is further decreased to 1, the main form of interaction switches from hydrogen bonding to protonation or the formation of the pyridinium ions. The proportion of protonated imine groups increases to 19%, while that of imine groups involved in hydrogen bonding is reduced to 14%.

4 Conclusion

A new graft copolymer, 4VP-*g*-PVDF, was successfully synthesized through the molecular graft copolymerization of 4VP with an ozone-preactivated PVDF backbone in NMP solution. The MF membranes prepared from 4VP-*g*-PVDF copolymers of different graft concentrations by the phase inversion technique in water showed enrichment of the hydrophilic 4VP polymer on the surface. The mean pore size of the 4VP-*g*-PVDF MF membranes increased with an increasing 4VP polymer graft concentration, a decreasing pH value of the casting bath, and a decreasing concentration of the casting solution. The flux of the aqueous solution through the 4VP-*g*-PVDF MF membranes exhibited a strong dependence on solution pH in the pH range 1–6, arising from the interaction of the grafted 4VP polymer on the pore surface with the aqueous solution through hydrogen bonding and protonation. The present study has shown that molecular functionalization by graft copolymerization prior to membrane fabrication is a relatively simple and effective approach to the preparation of membranes with well-controlled pore size, uniform surface composition (including the composition of pore surface), and pH-sensitive flux properties.

References

1 K. Li, *Chem. Eng. Technol.*, 2002, **25**, 2.
2 B. Mattsson, H. Ericson, L. M. Torell and F. Sundholm, *J. Polym. Sci., A: Polym. Chem.*, 1999, **37**, 3317.
3 W. S. Kim, T. Tanaka, H. Kumura and K. Shimazaki, *Biochem. Cell Biol.*, 2002, **80**, 91.
4 T. Uragami, M. Fujimoto and M. Sugihara, *Polymer*, 1981, **22**, 240.
5 A. Bottino, G. Capannelli and S. Munari, *J. Appl. Polym. Sci.*, 1985, **30**, 3009.
6 S. Masaharu, *Japan Pat.*, JP 08299770 A2, Nov. 1996.
7 J. Sirohi and I. Chopra, *J. Intell. Mater. Syst. Struct.*, 2001, **11**, 246.
8 L. F. Brown and G. R. Harris, *IEEE Trans. Ultrason., Ferroelectr., Freq. Control*, 2000, **47**, 1275.
9 B. Mazurek, T. Janiczek and J. Chmielowiec, *J. Electrost.*, 2001, **51**, 76.
10 N. P. Chen and L. Hong, *Polymer*, 2002, **43**, 1429.
11 R. Y. M. Huang, R. Pal and G. Y. Moon, *J. Membrane Sci.*, 2000, **167**, 275.
12 M. C. Porte-Durrieu, C. Aymes-Chodur, N. Betz and C. Baquey, *J. Biomed. Mater. Res.*, 2000, **52**, 119.
13 S. Han, W. K. Choi, K. H. Yoon and S. K. Koh, *J. Appl. Polym. Sci.*, 1999, **72**, 41.
14 M. Muller and C. Oehr, *Surf. Coat. Technol.*, 1999, **119**, 802.
15 Y. M. Lee and I. K. Shim, *J. Appl. Polym. Sci.*, 1996, **61**, 1245.
16 P. Wang, K. L. Tan, E. T. Kang and K. G. Neoh, *J. Membrane Sci.*, 2002, **195**, 103.
17 T. Lehtinen, G. Sundholm and F. Sundsolm, *J. Appl. Electrochem.*, 1999, **29**, 677.
18 T. Tarvainen, T. Nevalainen, A. Dundell, B. Svarfvar, J. Hyrsyla, P. Paronen and K. Jarvinen, *J. Controlled Release*, 2000, **66**, 19.
19 L. Fan, J. L. Harris, F. A. Roddick and N. A. Booker, *Water Res.*, 2001, **35**, 4455.
20 S. Hietala, S. L. Maunu and S. Sundholm, *Macromolecules*, 1999, **32**, 788.
21 J. F. Hester, P. Banerjee and A. M. Mayes, *Macromolecules*, 1999, **32**, 1643.
22 S. P. Nunes, M. L. Sforca and K. V. Peinemann, *J. Membrane Sci.*, 1999, **106**, 49.
23 L. Ying, P. Wang, E. T. Kang and K. G. Neoh, *Macromolecules*, 2002, **35**, 673.
24 B. Boutevin, J. J. Robin, N. Torres and J. Casteil, *Polym. Eng. Sci.*, 2002, **42**, 78.
25 Y. G. Ko, Y. H. Kim, K. D. Park, H. J. Lee, W. K. Lee, H. D. Park, S. H. Kim, G. S. Lee and D. J. Ahn, *Biomaterials*, 2001, **22**, 2115.
26 H. Suh, Y. S. Hwang, J. E. Lee, C. D. Han and J. C. Park, *Biomaterials*, 2001, **22**, 219.
27 T. Fargere, M. Abdennadher, M. Delmas and B. J. Boutevin, *J. Polym. Sci., A: Polym. Chem.*, 1994, **32**, 1337.
28 H. I. Unal and O. Sanli, *J. Appl. Polym. Sci.*, 1996, **62**, 1165.
29 E. W. Washburn, *Proc. Natl. Acad. Sci. U.S.A.*, 1921, **7**, 115.
30 S. R. Tonge and B. J. Tighe, *Adv. Drug Deliver. Rev.*, 2001, **53**, 109.
31 M. L. Xiang, M. Jiang, Y. B. Zhang, C. Wu and L. X. Feng, *Macromolecules*, 1997, **30**, 2313.
32 M. Urzua, L. Gargallo and D. Radic, *J. Appl. Polym. Sci.*, 2002, **84**, 1245.
33 H. Jiao, S. H. Goh and S. Valiyaveettil, *Langmuir*, 2002, **18**, 1368.

34 L. Houben, K. Schoone and G. Maes, *Vib. Spectrosc.*, 1996, **10**, 147.
35 X. Zhou, S. H. Goh, S. Y. Lee and K. L. Tan, *Polymer*, 1998, **39**, 3631.
36 S. Schlucker, M. Heid, R. K. Singh, B. P. Asthana, J. Popp and W. Kiefer, *Z. Phys. Chem.*, 2002, **216**, 267.
37 K. L. Tan, B. T. G. Tan, E. T. Kang and K. G. Neoh, *J. Mol. Electron.*, 1990, **6**, 5.
38 Y. Liu, S. H. Goh, S. Y. Lee and C. Huan, *Macromolecules*, 1999, **32**, 1967.
39 L. Li, C. M. Chan, L. T. Weng, M. L. Xiang and M. Jiang, *Macromolecules*, 1998, **31**, 7248.